

The Influence of Johnson-Cook Parameters on SPH Modeling of Orthogonal Cutting of AISI 316L

Alaa A. Olleak¹, Mohamed N.A. Nasr², Hassan A. El-Hofy¹

¹ Department of Industrial Engineering and Systems Management, Egypt-Japan University of Science and Technology, Alexandria, Egypt

² Department of Mechanical Engineering, Faculty of Engineering, Alexandria University, Alexandria, Egypt

1 Abstract

Over the past few decades, there has been a growing interest in modelling of machining processes. In this regard, smoothed particle hydrodynamics (SPH) is one of the latest methods used for that purpose. SPH is a powerful technique that can be used in handling problems of large deformation that are difficult to be tackled using traditional finite element methods. The current work aims to present and evaluate the use of SPH in modelling the machining process. A coupled thermo-mechanical analysis of a 3D model is performed using LS-DYNA to predict the cutting forces and residual stresses during orthogonal cutting of AISI 316L, at different sets of machining conditions. The Johnson-Cook material constitutive model is used to simulate the material behavior. The simulation results are validated by a previously published experimental work and compared to finite element model.

2 Introduction

Stainless Steel 316L is widely used where high corrosion resistance and oxidation resistance are required such as pumps, valves, watches and marine applications. However, the high ductility of these steels works against their machinability. AISI 316L alloy has poor machinability compared to regular carbon steel since it tends to work harden if machined too quickly. High cutting speeds can cause tool wear or tool failure. Therefore, low speeds and constant feed rates are recommended for such alloy.

A great interest has been growing in using finite element (F.E.) methods in modelling of machining processes. The common approaches that have been used for that purpose are Lagrangian, Eulerian and Arbitrary Lagrangian-Eulerian (A.L.E.). The Eulerian approach handles the material flow around the tool without defining a failure criterion. However, the chip morphology has to be known before the simulation and this approach is not able to predict the residual stresses (R.S.) since it does not consider the elastic behavior of the material [1]. While by using the Lagrangian approach, a failure criterion or predefined failure line or surface must be defined and a very fine mesh is required to avoid mesh distortion problems. The A.L.E. method combines the advantages of both Lagrangian and Eulerian techniques [1]. Another advanced technique used in DEFORM software, called remeshing-rezoning, by which the element is deleted with all its parameters once it reaches a specific damage value, and then new elements are added to smooth the rough boundary produced by element deletion [2]. Recently, mesh-free methods were employed in large deformation problems. The most common mesh-free methods are Smoothed Particles Hydrodynamics (SPH) and Element-Free Galerkin (EFG). The mesh-free methods are able to handle large material distortion problems that are difficult to be handled using traditional F.E. techniques. Moreover, these methods can deal with moving discontinuities such as crack propagation simulations. However, these methods require higher CPU time than other traditional methods [3].

The SPH, a developing, mesh-free, adaptive, and Lagrangian method, was able to overcome the difficulties of metal cutting simulations in a report published by Heinstein in 1997 [4]. The method was developed by Gingold and Monaghan [5] and Lucy [6] to be used in astrophysics. SPH was then used for fluid flow problems governed by Navier-Stokes equations. The use of SPH was extended to solid mechanics by Libersky and Petschek in 1991 [7]. For modelling machining processes, Limido et al. [8] developed a 2D cutting model using SPH for both the workpiece and the tool. Villumsen et al. [9] developed a 3D orthogonal cutting model for Al 6082-T6 alloy. The study investigated the effect of SPH particles resolution, mass scaling, time scaling, and coefficient of friction on cutting and thrust force components. Espinosa et al. [10] developed a 3D model for high speed orthogonal cutting of Al 6061-T6. Calamaz et al. [11] predicted the effect of tool wear in orthogonal cutting of Ti6Al4V alloy on cutting forces. Madaj [12] developed a 3D model of low thickness using SPH and multiplied the predicted forces by the ratio between the real thickness and the developed model thickness. Xi et al. [13] developed both 2D and 3D models to study the influence of workpiece temperature on cutting

Ti6Al4V alloy. Demiral [14] studied the influence of vibration parameters on the cutting forces while vibration-assisted turning of Ti6Al4V alloy. Xi et al. [15] studied the effect of laser assistance while turning of Ti6Al4V alloy.

The work in which the thrust forces are predicted using SPH and validated is very limited. Espinosa's model [10] underestimated the thrust forces by 30%. Calamaz model [11] underestimated the thrust force components for four sets of Johnson-Cook parameters with minimum difference of 35% and maximum difference of 42%. However, they assumed that the tool velocity is ten times higher than the real velocity. Furthermore, they used 2D models and the contact algorithm for 2D in LS-DYNA does not consider any frictional parameters [16]. The choice of the analysis type is important since Villumsen [9] found that the thrust forces increase as the cutting speed increases using mechanical analysis only without taking the thermal parameters in consideration, which is contradictory to the real case.

The residual stresses (R.S.) effect on the performance of the machined components, especially of material with high corrosion resistance, is significant. The R.S. affect the fatigue life, corrosion resistance and strength. Therefore, understanding the R.S. is of crucial importance. Outeiro et al. [17] measured the R.S. for AISI 316L at cutting speed 200 m/min and uncut chip thickness of 0.1 mm. Umbrello et al. [18] predicted the R.S. for the same material and cutting conditions using five different Johnson-Cook parameters using F.E. techniques. Nasr et al. [1] predicted the R.S. using A.L.E. method for exactly the same material used here. There is no work found in the literature in which R.S. are predicted using SPH method.

The current study aims to re-evaluate the use of SPH technique in modelling of machining and extend its use to R.S. prediction. A thermo-mechanical analysis of orthogonal cutting of AISI 316L using SPH technique is proposed. The results are validated by the experimental results in [17], and compared to F.E. simulations results in [18]. Johnson-Cook material constitutive model is used since it is well suited for simulating materials subjected to large strains, high strain rates, and high temperatures [19]. No damage criteria has to be defined when using SPH. However, the damage models was previously adopted to accurately predict the chip morphology in [12].

2.1 SPH Method

In SPH, the domain (Ω) is represented by a set of particles; each particle carries the field variable and interacts with other particles within a range controlled by the support domain S , Fig. 1. The field variable for any particle i within the domain is interpolated using the same field variables for the other particles that fall within the support domain. The support domain size is controlled by the smoothing length h , which varies in time and space in with the aim of partitioning the domain into boxes, each box represents the support domain.

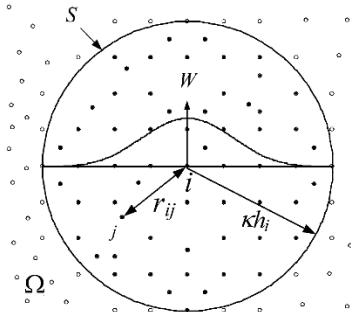


Fig. 1: SPH particle approximations in a two-dimensional problem domain, with a surface S . [3]

After representing the system by set of particles, the integral representation for the domain, known as kernel approximation, by which the particles are interpolated, is generated. The Kernel approximation for any two particles in the domain i and j is given by

$$f(x_i) = \int_{\Omega} f(x_j) W(x_i - x_j, h) dx_j \quad (1)$$

While W is the smoothing kernel function, given by equation 2. This approximation is performed to all terms related to field functions to produce a set of partial differential equations that can be solved using explicit integration algorithms.

$$W(x_i - x_j, h) = \frac{1}{h(x_i - x_j)^d} \theta(x_i - x_j) \quad (2)$$

Where θ is the interpolation function, and d is number of space dimensions. The smoothing function should be an even and centrally peaked function as shown in Fig. 2. The most common interpolation function used in the smoothing kernel function is cubic B spline function $\theta(r)$, given by

$$\theta(u) = \kappa \begin{cases} 1 - \frac{3}{2}u^2 + \frac{3}{4}u^3 & |u| \leq 1 \\ \frac{1}{4}(2-u)^3 & 1 \leq |u| \leq 2 \\ 0 & |u| \geq 2 \end{cases} \quad (3)$$

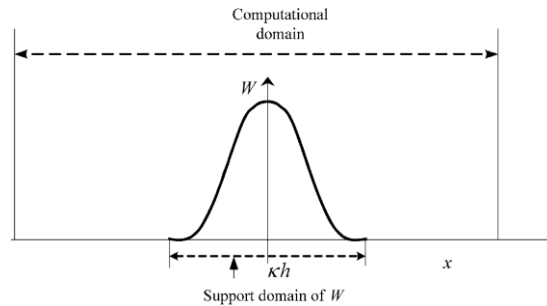


Fig. 2: The kernel smoothing function for a support domain located within the problem domain. [3]

For finite number of particles N , the continuous form of kernel approximation can be written in a discretized form as

$$f(x_i) = \sum_{j=1}^N \frac{m_j}{\rho_j} f(x_j) W(x_i - x_j, h) \quad (4)$$

The previous equation can be similar in form to F.E. formulation by considering the term $m_j/\rho_j W(x_i - x_j, h)$ as the SPH shape function. However, the shape function of SPH behaves differently from F.E. shape functions since it does not satisfy Kronecker delta function. Furthermore, the SPH shape function has to be constructed only for the particle of interest i , and as the location of the particle of interest changes, a different shape function is constructed. As a result, the construction of shape function has to be performed during the analysis, and therefore, a high computational time will be required.

The computational time of the SPH method is about 1.1 to 50 times higher than F.E. methods. However, in terms of ratio of accuracy to computational time, the SPH method is superior, especially for high deformation problems.

3 Model Description

3.1 Machining Conditions

A tool of rake angle 0° , clearance angle 11° , and edge radius of $30 \mu\text{m}$ is used for dry cutting of AISI 316L round bars. The cutting speeds are 100-200 m/min, the uncut chip thickness is 0.1-0.2 mm, and the width is 6 mm. These conditions are selected according to the cutting conditions used in a previously published experimental work [17].

3.2 Model Assumptions

A 3D SPH model is used to predict both cutting forces and R.S. in the machined surface of the workpiece. The tool is assumed rigid and fixed in all directions except the cutting direction. The cutting distance is set to 10 mm to achieve the steady state condition, the width to 0.05 mm to reduce the computational time, and the height to 1 mm, Fig. 3. A traditional F.E. mesh is used to represent the tool and SPH particles are used to represent the workpiece. The spacing between SPH particles is set to $20 \mu\text{m}$. Although this resolution is not high enough to correctly predict the chip morphology, it is suitable to get a converged solution as a function of the particles spacing [9]. The total number of particles is 32,000. The lowest particles of the workpiece are fixed in all directions.

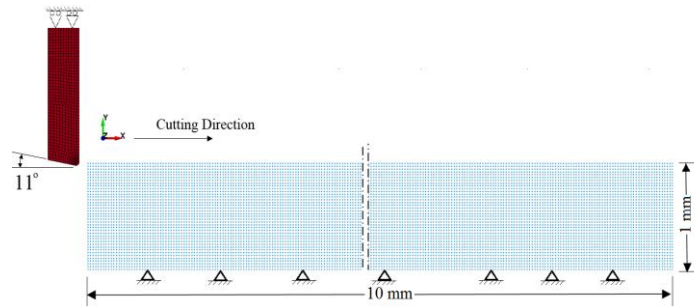


Fig. 3: SPH cutting model

3.3 Material Constitutive Model

Johnson-Cook material constitutive model [19] represented in equation 5 is used to simulate the material behavior.

$$\sigma_{flow} = [A + B\epsilon^n][1 + C \ln(\dot{\epsilon}/\dot{\epsilon}_o)][1 - (\frac{T - T_R}{T_M - T_R})^m] \quad (5)$$

Where A is the initial yield strength, B and n represent the effect of strain hardening, C is the strain rate sensitivity constant, m is the thermal softening exponent, ϵ is the plastic strain, $\dot{\epsilon}$ is the strain rate, $\dot{\epsilon}_o$ is the reference strain rate, T is the workpiece temperature, T_R is the reference temperature, and T_M is the melting temperature. Five Johnson-Cook parameters measured by different means used in [18] were selected to be used in this study with the aim of studying the influence of them on the SPH model results, Table 1. The mechanical and thermal properties of the workpiece material and the tool are listed in Table 2.

In LS-DYNA, in order to use Johnson-Cook material constitutive model, an equation of state (EOS) is required [21]. The EOS is a mathematical description of the material behaviour for a given set of initial conditions. There are two types of EOS can be used for solids; Gruneisen and Linear Polynomial [21]. The equation of state type has a remarkable effect on the results. Gruneisen EOS is recommended for high speeds and its parameters are not available for AISI 316L [22]. Therefore, the simplified linear polynomial EOS, given in equation 6, is used. The hydrostatic pressure is given by:

$$P = K\mu \quad (6)$$

Where μ is the compression ratio, and K is the bulk modulus [21].

	A(MPa)	B(MPa)	C	n	m	
M1 [23]	305	1161	0.01	0.61	0.517	1
M2 [23]	305	441	0.057	0.1	1.041	1
M3 [24]	301	1472	0.09	0.807	0.623	0.001
M4 [25]	280	1750	0.1	0.8	0.85	200
M5 [26]	514	514	0.42	0.508	0.533	0.001

Table 1: Johnson-Cook parameters for AISI 316L

		Tool	Workpiece
Material		WC/Co	AISI 316L
Density	Kg/m ³	15,250	8000
Young's modulus	GPa	600	193
Poisson's ratio		0.21	0.27
Melting temperature	°C	-	1375
Specific heat	J/Kg. °C	-	500
Thermal conductivity	W/m-K	-	16.3
Thermal expansion coefficient	m/m.K	-	17.2 x 10 ⁻⁶

Table 2: Mechanical and thermal properties of workpiece and tool materials [17, 27]

3.4 Friction Modelling

The simple Coulomb's law was considered on the whole contact zone. By using Coulomb law, the ratio between the frictional stress to the normal stress or between the thrust force to the cutting force is assumed constant. Even though this is a simplistic approach, it has been widely used in metal cutting simulations [1, 29, 31, 32]. In order to investigate the effect of friction coefficient (μ) on the process, different values ranging from 0.2 to 0.8 were used. This approach was previously adopted in [33].

For 2D FE/SPH, 2D SPH/SPH, or 3D SPH/SPH contacts, no friction coefficient has to be defined and the friction is directly managed by the interaction of the particles that result from the three conservative equations. Calamaz et al. [11] conducted a study to measure the equivalent Coulomb friction coefficient using SPH/SPH cutting model for different cutting speeds. They proved that the equivalent Coulomb friction parameter evolves slowly with the relative speed and the maximum value he could reach was 0.27. Therefore, using SPH/SPH models is not efficient for applications in which high friction occurs.

3.5 Thermal Parameters

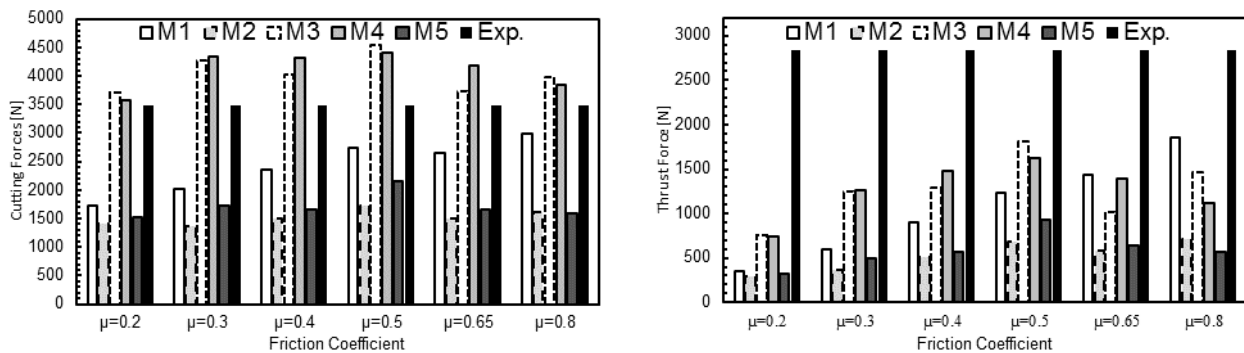
The thermal parameters for the workpiece materials are listed in Table 2. When using SPH method, the contact algorithm in LS-DYNA does not allow the heat transfer between the SPH part and the tool, or between the SPH part and the surrounding. Therefore, the process is assumed adiabatic and the workpiece cannot be cooled to the room temperature, which may affect the predictions accuracy. However, this assumption can be valid as (1) most of the heat is carried away by the chip, (2) the SPH part in the workpiece is large enough to dissipate the heat, and (3) the expansion coefficient is set to zero. Taylor Quinney coefficient, the fraction of plastic work converted into heat, is assumed 0.9 [1, 28, 29, 30].

4 Results

4.1 Cutting Forces

The predicted cutting and thrust forces for each set of Johnson-Cook parameters and friction coefficient are shown in Fig. 4. Accordingly, it can be noticed that sets M2 and M5 are highly underestimating the forces. This high underestimation can be a result of their low strain hardening constants compared to the other sets of material parameters. This assumption can be supported by their higher damage values used in [18]. Furthermore, the constants of M5 were identified through machining tests in which the flow stress match with the stress at primary shear zone based on cutting forces results [26]. The constants of M1 and M2 were identified using both results from Split Hopkinson's Bar (SHPB) tests and from orthogonal slot milling experiment. On the other hand, the sets M3 and M4 constants were identified only through experiments using SHPB tests [18]. Moreover, it is noticed in the literature that Johnson-Cook parameters identified through SHPB tests are widely used in SPH models [8, 11, 13, and 15].

From Fig. 4, it is obvious that the least difference between the predicted and measured cutting forces can be achieved at friction coefficient of 0.2 for M3 and M4 (2% and 6% respectively), and 0.8 for M1. However, for thrust forces, the least difference can be achieved at friction coefficient of 0.8 for sets M1, M3, and M4. After excluding the results of M2 and M5, the average difference between the predicted forces and the measured forces at $\mu=0.8$ is 13% for the cutting forces, and 48% for the thrust forces. The best prediction is given by M1 parameters. Fig. 5 shows the influence of the friction coefficient on the ratio between the thrust forces to the cutting forces (Equivalent friction coefficient). This ratio is supposed to be equal to the friction coefficient, which does not occur at high friction coefficient values. The main reason of this difference is that, at high friction coefficient values, some particles of the SPH part stick on sliding region of the tool surface and do not allow other particles to slide on the tool surface where they stick.



(a) Cutting force

(b) Thrust force

Fig. 4: Comparison between predicted and measured forces for different sets of Johnson-Cook parameters and friction coefficient

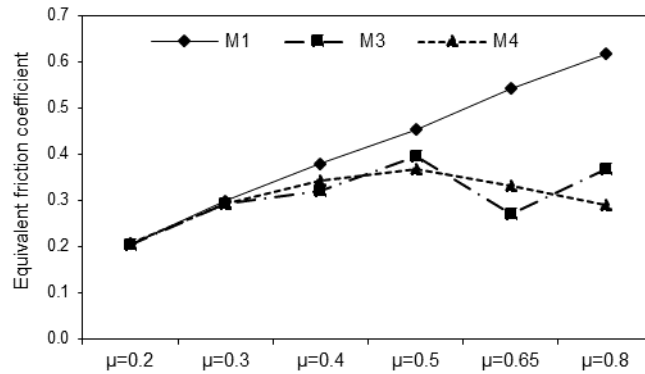


Fig. 5: Friction coefficient influence on the ratio between the thrust and cutting forces

A comparison between predicted DEFORM F.E. [18] and LS-DYNA SPH results is shown in Fig. 6. It is worth pointing out that, in F.E. simulations, the critical damage value D_{CR} of the three sets are equal, which makes this comparison more reasonable. It is obvious that DEFORM predictions are closer to the experimental results than LS-DYNA SPH. The cutting and thrust forces predicted by M3 are larger than that predicted by using M4 in both F.E. and SPH simulations. The accuracy of F.E. model lies behind the use of the Cockcroft and Latham fracture criterion, which is not adopted in the SPH model [2]. However, in LS-DYNA, it is possible to use Johnson-Cook or Cockcroft and Latham fracture models, but for the modified Johnson-Cook constitutive law [21].

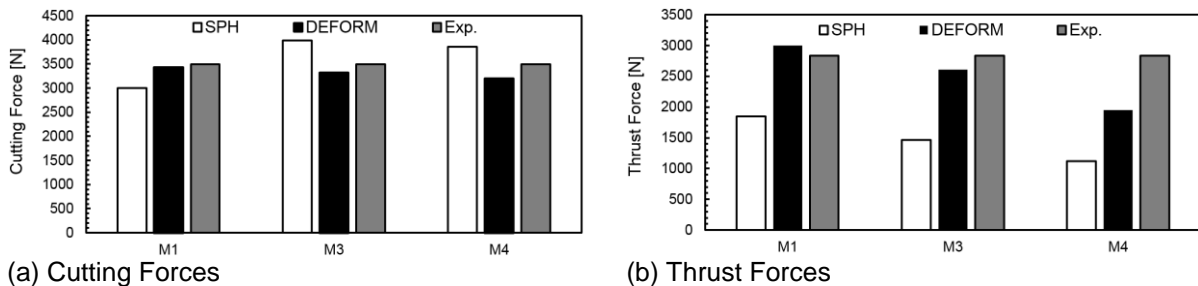


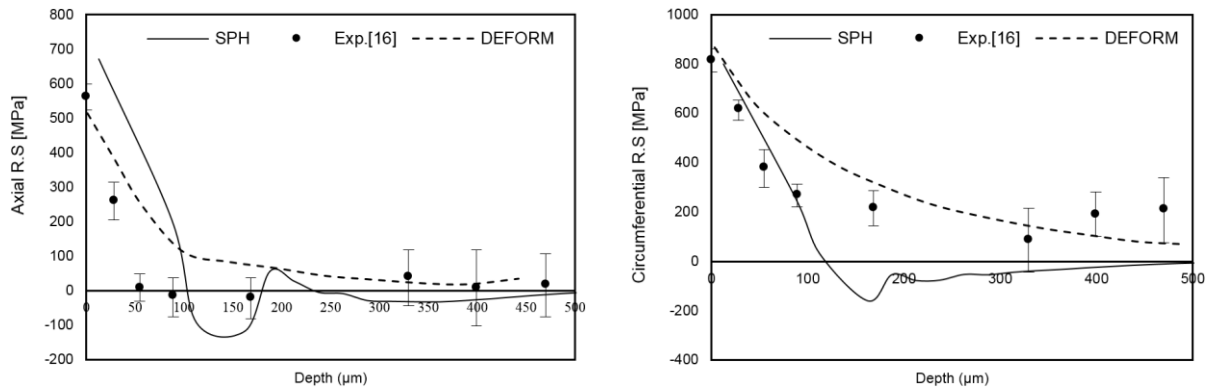
Fig. 6: Comparison between SPH, DEFORM and experimental results.

4.2 Residual Stresses

From Fig. 4, the best prediction is given by M1 parameters at friction coefficient of 0.8; therefore, these conditions are used in predicting the R.S. for cutting speed 200 m/min and uncut chip thickness of 0.1 mm. The average R.S. are taken at the middle of the workpiece for 160 particles at every depth (total of 3,200 particles). The minimum depth below the machined surface is 12.5 μm and the R.S. at the surface is measured at this depth. Because most of the SPH particles below the machined surface are displaced, the R.S. are calculated according to their initial location. The particle with high displacement and abnormal results are excluded and the number of the particles considered for R.S. calculations is reduced to 2750.

Fig. 7 (a) shows the axial R.S. predicted by SPH compared to that measured from experiments and that predicted by F.E. results by DEFORM [18]. In SPH, the mean value of the axial R.S. is overestimated at the machined surface and the first 100 μm of the depth. Furthermore, the SPH model could predict a tensile layer that is larger than that was measured experimentally, which was not predicted by the F.E. model. After the first 100 μm , the predicted results fall within the range of values measured from the experiments.

In Fig. 7 (b), the predicted circumferential R.S. is in good agreement with the measured values within the first 100 μm . After this depth, the circumferential R.S. become compressive and a tensile layer is predicted, and then stabilizing to zero, which is not the case in measurements and F.E. model. This difference between the predicted and experimental values can be a result of the friction model problems, adiabatic assumption, and material modelling which already have influence on the cutting forces results.



(a) Axial R.S.

(b) Circumferential R.S.

Fig. 7: Comparison between experimentally and numerically obtained residual stresses.

5 Summary

- A numerical analysis of cutting forces and residual stresses induced by orthogonal cutting of AISI 316L was performed using SPH method. The predicted results of SPH simulations show good correlation with the experimental results for M3 and M4. Therefore, in order to have accurate results, the choice of the Johnson-Cook constants is of crucial importance. Johnson-Cook constants identified experimentally from Split Hopkinson's Bar tests should be used while using SPH.
- The SPH method was underestimating the feed forces at high friction coefficients. Therefore, it is recommended to use the SPH method for applications in which the ratio between the thrust and cutting forces is low. A further detailed investigation on the frictional behavior in FE/SPH and SPH/SPH contacts should be conducted to correctly predict the cutting forces over wide range of machining conditions. On the other hand, the frictional behavior in 2D FE/SPH, 2D SPH/SPH, and 3D SPH/SPH contacts should be developed to include another friction models.
- The future work will be focused on fully 3D SPH models in turning, milling and drilling operations.

6 Acknowledgement

This research project is sponsored by ELARABY GROUP Graduate Scholarship to the Egypt Japan University of Science and Technology (E-JUST) and support of the Japanese International Cooperation Agency (JICA).

7 Literature

- [1] Nasr MNA, Ng. EG, Elbestawi MA. Modelling the effects of tool-edge radius on residual stresses when orthogonal cutting AISI 316L. *International Journal of Machine Tools & Manufacture*. 2007; 47(2): p. 401-411.
- [2] Umbrello D. Finite element simulation of conventional and high speed machining of Ti6Al4V alloy. *Journals of Material Processing Technology*. 2008; 196(1-3): p. 79-87.
- [3] Liu GR. *Meshfree methods: moving beyond the finite element method*: CRC Press; 2010.
- [4] Heinstein M, Sagalman D. *Simulation of Orthogonal Cutting with Smooth Particle Hydrodynamics*. Livermore, California, USA; 1997.
- [5] Gingold R, Monaghan J. Smoothed particles hydrodynamics: theory and application to non-spherical stars. *Monthly Notices of the Royal Astronomical Society*. 1977; 181: p. 375-89.
- [6] Lucy L. A numerical approach to the testing of fusion process. *Astronomical Journal*. 1977; 82: p. 1013-24.
- [7] Libersky L, Petschek A. Smooth particle hydrodynamics with strength of materials. *Proceedings of the Next Free-Lagrange Conference Held at Jackson Lake Lodge*. 1991;: p. 248-257.
- [8] Limido J, Espinosa C, Salaun M, Lacomme J. SPH method applied to high speed cutting modelling. *International Journal of Mechanical Sciences*. 2008; 49(7): p. 898-908.
- [9] Villumsen M, Fauerholdt T. Simulation of metal cutting using smooth particle hydrodynamics. In *7th LS-DYNA Anwenderforum*; 2008; Bamberg.
- [10] Espinosa C, Lacomme J, Limido J, Salaun M, Mabru C, Chieragatti R. Modeling high speed machining with the SPH method. In *10th International LS-DYNA users conference*; 2008; Dearborn, Michigan USA.

- [11] Calamaz M, Limido J, Nouari M, Espinosa C, Coupard D, Salaun M, et al. Toward a better understanding of tool wear effect through a comparison between experiment and SPH numerical modelling of machining hard materials. *International journal of refractory metals and hard materials*. 2009; 27(3): p. 595-604.
- [12] Madaj M, Piska. On the SPH orthogonal cutting simulation of Al2024-T351 alloy. In *Procedia CIRP* 8; 2013; Turin, Italy: Elsevier Procedia. p. 152-157.
- [13] Xi Y, Bermingham M, Wang G, Dargusch M. SPH/FE modelling of cutting force and chip formation during thermally assisted machining. *Computational materials science*. 2014; 84(188-197): p. 188-197.
- [14] Demiral M. SPH modeling of vibro-assisted turning of Ti alloy: Influence of vibration parameters. *Journal of Vibroengineering*. 2014; 16(6): p. 2685-2694.
- [15] Xi Y, Zhan , Rashid , Wang , Sun , Dargusch M. Numerical modeling of laser assisted machining of a beta titanium alloy. *Computational Materials Science*. 2014; 92: p. 149–156.
- [16] LSTC. LS-DYNA Keyword User's Manual-Volume I Livermore, California: LSTC; 2014.
- [17] Outeiro JC, Umbrello D, M, Saoubi R. Experimental and numerical modelling of the residual stresses induced in orthogonal cutting of AISI 316L steel. *International Journal of Machine Tools & Manufacture*. 2006;: p. 1786-1794.
- [18] Umbrello D, M'Saoubi R, Outeiro JC. The influence of Johnson-Cook material constants on finite element simulation of machining of AISI 316L steel. *International Journal of Machine Tools & Manufacture*. 2007;: p. 462-470.
- [19] Johnson G, Cook H. A constitutive model and data for metals subjected to large strains, high strain rates and high temperatures. In *Proceedings of the seventh international symposium on ballistics*; 1983. p. 541–7.
- [20] M.B. Liu GRL. Smoothed particle hydrodynamics (SPH): an overview and recent developments. *Archives of computational methods in engineering*. 2010; 17(1): p. 25-76.
- [21] (LSTC) LSTC. LS-DYNA KEYWORD USER'S MANUAL: Material Models Livermore, California; 2014.
- [22] Zukas J. *Introduction to Hydrocodes* Baltimore, USA: ELSERVIER; 2004.
- [23] Chandrasekara H, M'Saoubia R, Chazalb H. Modelling of material flow stress in chip formation process from orthogonal milling and split hopkinson bar tests. *Machining Science and Technology: An International Journal*. 2005; 9(1): p. 131-145.
- [24] R.M'Saoubi. High-speed shear tests for the identification of the Johnson–Cook ENSAM-Paris: Ph.D Thesis; 1998.
- [25] Changeux B, Touratier M, Lebrun J, Thomas T, Clisson J. High-speed shear tests for the identification of the Johnson-Cook law. In *Fourth International ESAFORM Conference on Lie`ge*; 2001; Belgium.
- [26] Tounsi N, Vincenti J, Otho A, Elbestawi MA. From the basic mechanics of orthogonal metal cutting toward the identification of the constitutive equation. *International Journal of Machine Tools and Manufacture*. 2002; 42(12): p. 1373–1383.
- [27] Harvey PD. *Engineering Properties of Steels* Metals Park, OH: ASM International; 1982.
- [28] Shet C, Deng X. Finite element analysis of the orthogonal metal cutting process. *Journal of Materials Processing Technology*. 2000; 105(1-2): p. 95–109.
- [29] M. Nasr, E.-G. Ng & M. Elbestawi, 2007, "Effects of Strain Hardening & Initial Yield Strength on Machining-induced Residual Stresses", *J. of Engineering Materials & Tech., Trans. of the ASME*, 129 (4), pp. 567-579
- [30] M. Nasr, E.-G. Ng & M. Elbestawi, 2007, "Effects of Workpiece Thermal Properties on Machining-induced Residual Stresses – Thermal Softening & Conductivity", *J. of Engineering Mfg., Proceedings of the IMechE, part B*, 221 (9), pp. 1387-1400.
- [31] L. Chen, T.I. El-Wardany, M. Nasr & M. Elbestawi, 2006, "Effects of Edge Preparation & Feed when Hard Turning a Hot Work Die Steel with Polycrystalline Cubic Boron Nitride Tools", *Annals of the CIRP*, 55 (1), pp. 89-92.
- [32] Arrazola PJ, Ozel T, Umbrello D, Davies M, Jawahir IS. Recent advances in modelling of metal machining processes. *CIRP Annals- Manufacturing Technology*. 2013; 62(2): p. 695-718.
- [33] Filice L, Micari F, Rizzuti S, Umbrello D. A critical analysis on the friction modelling in orthogonal machining. *International Journal of Machine Tools & Manufacture*. 2007; 47(3–4): p. 709–714.